A Novel Exosite on Coagulation Factor VIIa and Its Molecular Interactions with a New Class of Peptide Inhibitors‡

Martin Roberge,§ Lydia Santell,§ Mark S. Dennis,§ Charles Eigenbrot, Mary A. Dwyer,|| and Robert A. Lazarus*

Department of Protein Engineering, Genentech, Inc., 1 DNA Way, South San Francisco, California 94080

Received March 23, 2001; Revised Manuscript Received June 8, 2001

ABSTRACT: A new inhibitory peptide binding exosite on the protease domain of coagulation Factor VIIa (FVIIa) has been identified. A novel series of peptide inhibitors of FVIIa, termed the "A-series" peptides, identified from peptide phage libraries and exemplified by peptide A-183 [Dennis, M. S., Roberge, M., Quan, C., and Lazarus, R. A. (2001) *Biochemistry 40*, 9513−9521], specifically bind at a site that is distinct from both the active site and the exosite of another recently described peptide inhibitor of FVIIa, E-76 [Dennis, M. S., Eigenbrot, C., Skelton, N. J., Ultsch, M. H., Santell, L., Dwyer, M. A., O'Connell, M. P., and Lazarus, R. A. (2000) *Nature 404*, 465-470]. Peptide A-183 prolonged TF-dependent clotting in human, but not rabbit plasma. Thus, a panel of human FVIIa mutants, containing 70 of the 76 rabbit sequence differences in the protease domain, localized the binding site to residues in the 60s loop and the C-terminus. The location of the exosite was refined by a series of FVIIa alanine mutants, which showed that proximal residues Trp 61 and Leu 251 were critical for binding. Kinetic and equilibrium binding constants for zymogen FVII, FVIIa and TF·FVIIa were determined using immobilized N-terminal biotinylated A-183 by surface plasmon resonance. No peptide binding to nine other human serine proteases was observed. Key residues on the peptide were determined from binding to FVIIa and inhibition of FX activation using a series of alanine mutants of A-183 fused to the Z domain of protein A. Analysis of the mutagenesis data is presented in the context of a crystal structure of A-183 in complex with a version of zymogen FVII [Eigenbrot, C., Kirchhofer, D., Dennis, M. S., Santell, L., Lazarus, R. A., Stamos, J., and Ultsch, M. H. (2001) *Structure 9*, 627−636]. The shape and proximity of this exosite to the active site may lend itself towards the design of new anticoagulants that inhibit FVIIa.

Enzymes catalyze reactions by lowering the activation barrier for transformation of a substrate to a product. Inherent in the nature of enzymes is the active site—the region of an enzyme that encompasses the residues involved in the catalytic machinery. Enzymes that catalyze similar reactions are generally part of an enzyme family having similar structural features and, in particular, similar active sites. Serine proteases catalyze the hydrolysis of peptide bonds and are one of the best studied enzyme families. They are divided into two major subfamilies, the chymotrypsin family and the subtilisin family (*1*−*4*). Both of these subfamilies rely upon the same active site amino acid residues to carry out their function, namely the serine, histidine, and aspartic acid residues that form the catalytic triad.

The catalytic domains of the chymotrypsin family of serine proteases are highly homologous (*1*−*3*). While some members of this family such as trypsin and chymotrypsin are moderately nonselective in their substrate specificity, most other serine proteases have a relatively high degree of specificity (*3*). Contributing to substrate specificity are residues in the "substrate binding cleft" at the S and S′ subsites that, while distinct from the catalytic residues, still constitute part of the extended active site. The naturally occurring substrates for many serine proteases are themselves often large proteins and as such bring additional binding sites and complexity to the catalytic process.

Interest in modulating the effect of coagulation Factor VIIa (FVIIa),[1] a key serine protease in the coagulation cascade (*5*, *6*), has led to the development of inhibitors of this enzyme as potential anticoagulants (*7*−*11*). This is due to its importance in initiating the coagulation process (*12*, *13*) upon exposure to tissue factor (TF), an essential membrane bound cofactor for FVIIa (*14*). There are three macromolecular protein substrates for TF·FVIIa—zymogens Factor X (FX), Factor IX (FIX), and Factor VII (FVII)—which are cleaved to their activated forms. FVIIa, FIXa, and FXa are vitamin K-dependent glycosylated serine proteases that share a similar molecular architecture, being composed of an amino-terminal γ-carboxyglutamic acid-rich (Gla) domain, two epidermal growth factor (EGF)-like domains, and the chymotrypsin-like serine protease domain.

‡ The X-ray crystallographic coordinates of the A-183·rF7 complex have been deposited in the Protein Data Bank under accession code 1JBU.

* To whom correspondence should be addressed. Phone: (650) 225-1166. Fax: (650) 225-3734. E-mail: lazarus.bob@gene.com.

§ These authors contributed equally to this work.

|| Current address: Department of Biochemistry, Duke University, Durham, NC 27710.

[1] Abbreviations: TF, tissue factor; FVIIa, Factor VIIa; FIXa, Factor IXa; FXa, Factor Xa; BEGR-FVIIa, biotinylated Glu-Gly-Arg covalently bound to the FVIIa active site; E-76, Ac-ALCDDPRVDRWY-CQFVEG-NH_2; HEPES, *N*-2-hydroxylethylpiperazine-*N*′-2-ethanesulfonic acid; HRP, horseradish peroxidase; A-183, EEWEVLCWTWETCER; PT, prothrombin time; Z, consensus domain of protein A; rF7, a version of FVII containing only the EGF2 and protease domains.

10.1021/bi010592d CCC: $20.00
Published on Web 07/17/2001

Although the structure of a ternary TF·FVIIa·FX complex is not known, FX binding sites have been mapped onto the TF·FVIIa complex by mutagenesis and antibody competition studies. They include determinants on both the Gla and protease domains of FVIIa (*15*−*19*) and the carboxy-terminal type III fibronectin domain of TF (*20*−*23*), all of which are remote from the active site. In the case of FVIIa, studies of these so called "exosites", i.e., regions that are distinct from the active site yet play an important role in the molecular recognition of substrates and inhibitors, has led to a better understanding of both their function and mechanism (*24*, *25*).

In a previous study, we identified a new class of potent FVIIa inhibitors by selecting peptides from phage-displayed libraries (*10*). These "E-series" peptides bound to FVIIa at an exosite and inhibited FX activation by both steric and allosteric mechanisms. The E-peptide binding exosite was located via FVIIa domain swaps, FVIIa mutagenesis, calcium dependence, and ultimately, X-ray crystallography of the FVIIa·E peptide complex. Interestingly, the exosite on FVIIa was in a topographically similar region as exosite I in thrombin, the fibrinogen recognition exosite (*26*, *27*). In addition to binding fibrinogen, the thrombin receptor, thrombomodulin, and heparin cofactor II, thrombin exosite I is also the binding site for hirugen (*28*), a dodecapeptide inhibitor of thrombin derived from the carboxy terminal tail of the leech protein hirudin (*29*). Thrombin also contains a second exosite termed exosite II or the heparin binding exosite which also binds prothrombin fragment 2 (*26*, *27*).

In this paper, we report on the binding site for the "A-series" peptides, a new class of peptide inhibitors of TF·FVIIa, which were discovered by phage display (*30*). The A-series peptides bind at a new exosite on the protease domain of FVIIa, which is distinct from both the active site and the E-peptide binding exosite; it is also distinct from the topographical region corresponding to exosite II in thrombin (*26*, *27*). We also present data on the important binding determinants and characteristics of the A-series peptides and rationalize interactions of both the peptide and protein using the crystal structure of their complex. To our knowledge, this binding site represents a previously unknown exosite on serine proteases.

EXPERIMENTAL PROCEDURES

Phage Binding ELISA. Polyvalently displayed (g8) phage clone A-53 was tested for its ability to recognize immobilized TF, FVIIa, TF·FVIIa, TF·FVIIa containing 8 μM TF7I-C (*7*), or TF with active-site blocked FVIIa (BEGR-FVIIa). Proteins were immobilized as described previously (*10*); TF refers to TF_{1-219}. TF bound to BEGR-FVIIa was prepared by adding BEGRCK-06 (Haematologic Technologies, Inc., Essex Junction, VT) to TF·FVIIa following immobilization. Approximately 10^{11} phage displaying A-53 (SAEWEVLCWTWEGCGSVGLV) were added to each well in sorting buffer (50 mM HEPES, pH 7.2, 5 mM $CaCl_2$, 5 mM $MgCl_2$, 150 mM NaCl, 1 % bovine serum albumin). After 1 h, the microtiter plate was washed with sorting buffer and bound phage were detected with a HRP/Anti-M13 conjugate (Pharmacia Amersham Biotech, Piscataway, NJ). The amount of HRP bound was measured using ABTS/H_2O_2 substrate and monitoring the change in absorbance at 405 nm.

To investigate peptide inhibition of phage binding, serially diluted A-57 or E-58 peptides were added to plates coated with TF·FVIIa as above, followed by the addition of approximately 10^{11} phage monovalently displaying (g3) either A-57 (SEEWEVLCWTWEDCRLEGLE) or E-58 (EGTLCDDPRIDRWYCMFSGV). The microtiter plate was washed with wash buffer (50 mM HEPES, pH 7.2, 150 mM NaCl, 0.05% Tween 20) and bound phage were detected as above. Peptides were synthesized as previously described (*30*).

Production of Peptide-Z Fusions. Peptides expressed as fusions to the amino terminus of the Z consensus domain of protein A were secreted into the culture fluid from *Escherichia coli* 27C7. Oligonucleotides were designed to insert the coding sequence for the phage-peptides between the stII signal sequence and the Z domain in the plasmid pZCT (*31*). Mutants of A-100-Z (EEWEVLCWTWETCERGEGGGGSGG-Z) were constructed in pA-100-Z using Kunkel mutagenesis and verified by DNA sequencing. *E. coli* 27C7 expressing A-100-Z mutants were grown in phosphate limiting media and peptide-Z fusions were purified using an IgG affinity column as described for A-100-Z (*30*). Each mutant protein was quantified using a calculated extinction coefficient. Further analysis included FAB mass spectrometry and SDS-PAGE.

A-183b Peptide Binding Assay. Peptide A-183 (EEWEV-LCWTWETCER), obtained by trypsin digestion of A-100-Z (*30*) was specifically biotinylated at the amino terminus using NHS-biotin (Pierce Chemical, Rockford, IL) according to the manufacturer to generate A-183b. The ability of peptide-Z fusions to compete with A-183b for binding to FVIIa was monitored using a solid phase binding assay. Dilutions of A-100-Z mutants in sorting buffer were added to microtiter plates coated with FVIIa. A-183b (2.5 nM) was then added and the plate was incubated at room temperature for 1 h. The microtiter plate was washed with wash buffer and the A-183b bound to FVIIa was detected with Streptavidin/HRP. The amount of HRP bound was measured using ABTS (or TMB)/H_2O_2 substrate and monitoring the change at 405 nm (or 450 nm).

In experiments to determine the effect of Ca^{2+} or NaCl on binding, 10 nM A-183b was added to wells coated with FVIIa and the sorting buffer was modified to contain various concentrations of Ca^{2+} ranging from 0 to 10 mM or NaCl ranging from 0 to 1 M. Experiments to determine the effect of pH on binding also used 10 nM A-183b added to wells coated with FVIIa. The sorting buffer was modified so that HEPES was replaced with 25 mM low ionic strength buffers between pH 2.0 and 12.0 (Hampton Research, Laguna Niguel, CA).

TF·FVIIa Activity Assays. Assays characterizing the inhibition of the TF·FVIIa catalyzed activation of FX were performed as previously described (*10*).

Kinetic Analysis of FVII and FVIIa Binding to Peptides. Rate and equilibrium binding constants of FVII and FVIIa binding to peptide were obtained by surface plasmon resonance using a model 2000 BIAcore instrument (Biacore, Inc., Piscataway, NJ). Binding kinetics were performed in duplicate in 20 mM Tris, pH 7.5, 100 mM NaCl, 5 mM $CaCl_2$, and 0.01% Tween 20 at a flow rate of 10 μL/min following capture of N-terminal biotinylated A-183 on a streptavidin-derivatized sensor chip. Association of FVII, FVIIa, TF_{1-219}·FVII, or TF_{1-219}·FVIIa was monitored during injection of a series of concentrations ranging from 16 to

500 nM. Dissociation from the peptides was observed over 10 min. After each analysis, bound analyte was completely eluted with 10 mM HCl. The k_{on} was calculated from the concentration dependence of the association rate constant and the k_{off} was determined from the early portion of the dissociation phase following injection utilizing software provided by the manufacturer. The equilibrium binding constant, K_d, equals the ratio of k_{off}/k_{on}. When dissociation was measured in the presence of TF, the kinetics were analyzed in the presence of 10 μM TF_{1-219} to ensure that separation of TF from FVII did not influence the measurements. In addition, samples after dissociation from peptide were subjected to SDS−PAGE to confirm that FVII was still in the zymogen form.

Human serine proteases were tested for binding to A-183b on the streptavidin-derivatized sensor chip described above. Binding was assessed by individual injections of a single high concentration of each enzyme (in parentheses). Thrombin (350 μM), FXa (200 μM), FIXa (150 μM), FXIa (6.8 μM), activated protein C (90 μM), and plasmin (160 μM) were obtained from Haematologic Technologies, Inc. (Essex Junction, VT). Plasma kallikrein (5.7 μM) and FXIIa (5.8 μM) were purchased from Enzyme Research Laboratories (South Bend, IN). t-PA (14 μM) was from T. Lipari at Genentech, Inc.

FVIIa/FIXa Chimeric Proteins. Plasmids encoding FVII/FIX chimeric proteins (*32*) VII-EGF2/IX ($FVII_{light\ chain}$/$FIX_{protease}$) and IX-EGF2/VII ($FVII_{protease}$/$FIX_{light\ chain}$) were transiently transfected into 293 cells (ATCC CRL 1573). Proteins were captured using TF or a FVII antibody. Specific binding of monovalent phage displaying the peptide sequences from A-65 (WEVLCWTWETCER) or E-76 (Ac-ALCDDPRVDRWYCQFVEG-NH_2) were detected using HRP conjugate-anti-M13 (Amersham Pharmacia Biotech, Piscataway, NJ). E-76 peptide phage have a Val-Glu instead of the acetyl group at the N-terminus.

FVIIa Mutagenesis. Substitution of 14 selected rabbit sequences into the protease domain of human FVIIa by site-directed mutagenesis (*33*) was followed by expression in 293 cells, western blot analysis of FVII, and characterization of their ability to bind monovalently displayed A-65 and E-76 peptide phage. The corrected sequence of rabbit FVII has been deposited in GenBank, accession no. U77477 (*34*).

Site-directed mutagenesis was performed on human FVII DNA in plasmid pRKCT31 using the Kunkel method (*33*) and mutations were confirmed by DNA sequencing. Production of FVII mutants was achieved by transiently transfecting 293 cells. FVII concentration was quantified by a FVII ELISA. Briefly, expressed FVII was captured on a TF_{1-219} coated well. The well was washed and polyclonal rabbit anti-human FVII was incubated in the well for 1 h. The presence of FVII was dectected with a goat anti-rabbit IgG-HRP conjugate. Specific activities for FX activation by FVIIa mutants and subsequent inhibition of FX activation were determined essentially as described (*10*). Briefly, cell culture supernatants were added to 50 pM relipidated TF_{1-243} in 20 mM HEPES, pH 7.2, 5 mM $CaCl_2$, 150 mM NaCl, 0.1% PEG-8000 for 30 min at room temperature in the presence or absence of varying concentrations of A-183. FX (100 nM) was added to initiate the reaction, and aliquots were removed at various times and quenched by mixing with an equal volume of 50 mM EDTA. The rate of FX activation was determined by addition of Spectrozyme FXa to the quenched samples and measuring the change in absorbance at 405 nm. The specific activity of the FVIIa alanine mutants in the absence of A-183 was the same as that for wild-type FVIIa.

Clotting Assays. Prothrombin time (PT) assays were performed in citrated pooled normal plasmas (human or various animal species) as previously described (*10*). Clotting times were determined using an ACL 300 Automated Coagulation Analyzer (Coulter Corp., Miami, FL) using Innovin (human relipidated TF and Ca^{2+}) obtained from Dade International Inc. (Miami, FL) to initiate the PT.

X-ray Structure of A-183·rF7 Complex. The complete details of the crystallization, data collection, structure solution, and refinement are found in Eigenbrot et al. (*35*). The working and free *R*-values for data 35-2 Å are 20.4 and 22.7%, respectively.

RESULTS AND DISCUSSION

A-Series Peptides Bind to a Unique Exosite on FVIIa. Since sorting the A-series library was carried out against the TF·FVIIa complex (*30*), we first wanted to assess the specific protein responsible for enrichment. The initial polyvalent A-series peptide phage clone, A-53 (*30*), was tested for its ability to bind immobilized FVIIa, TF, TF·FVIIa, active-site blocked FVIIa (BEGR-FVIIa), or TF·FVIIa in the presence of saturating TF7I-C, a Kunitz domain active site inhibitor (*7*). We found that A-53 phage bound to FVIIa, TF·FVIIa, BEGR-FVIIa, and TF·FVIIa in the presence of TF7I-C; however, we could not detect any binding of A-53 phage to TF. This suggested that the A-peptide binding site resides on FVIIa, but at a site distinct from the active site. In addition, A-peptide phage could bind to a $FVII_{protease}$/$FIX_{light\ chain}$ chimera, but not to a $FVII_{light\ chain}$/$FIX_{protease}$ chimera suggesting that the binding site on FVIIa could be further localized to the 254-residue serine protease domain.

These results were similar to those obtained for the E-series of peptides derived from a CX_9C peptide phage motif (*10*). Although A-53 was derived from a CX_5C motif and bore no sequence similarity to E-76, we investigated whether these peptides were binding to the same site. Two phage clones were identified following soft randomization of the initially selected A-53 and E-56 sequences and peptides corresponding to these clones, designated A-57 and E-58, respectively, were synthesized. The peptides were tested for their ability to block either A-57 or E-58 monovalently displayed on phage from binding to immobilized TF·FVIIa. As expected, both peptides blocked phage bearing their corresponding sequence from binding to TF·FVIIa. By contrast, neither peptide was able to block phage bearing the other sequence (Figure 1). Thus, A-57 binds to the protease domain of FVIIa at an exosite that is distinct from the exosite utilized by the E-series peptides.

Location of the A-Peptide Binding Exosite. Previously, we showed that the recombinantly derived A-series peptide, A-183 (EEWEVLCWTWETCER), specifically prolonged the TF-dependent clotting time in normal human plasma as measured in the prothrombin time (PT) assay (*30*). Since we were interested in testing the anticoagulant effects of A-183 in vivo, we screened plasmas from several species to determine any species-dependent clotting effects. We found that A-183 also prolonged the PT in chimpanzee and baboon

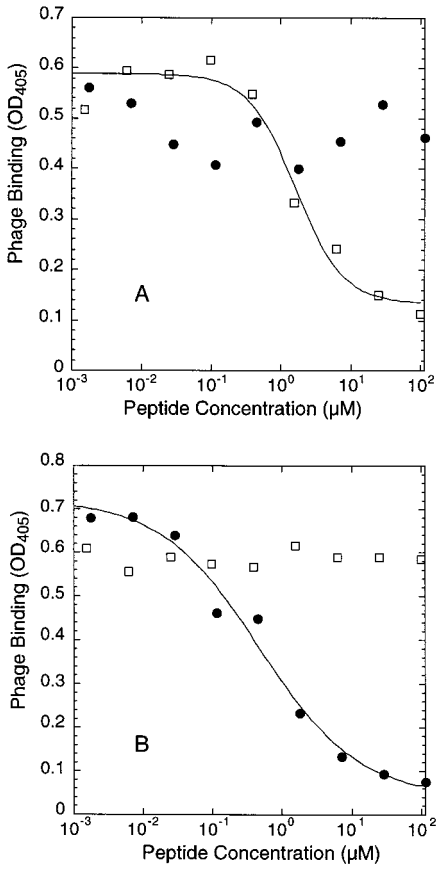

FIGURE 1: A-peptide and E-peptide phage bind to distinct exosites. (A) E-58 displaying phage are displaced from TF·FVIIa by peptide E-58 (□), but not peptide A-57 (●). (B) A-57 displaying phage are displaced from TF·FVIIa by peptide A-57 (●), but not peptide E-58 (□).

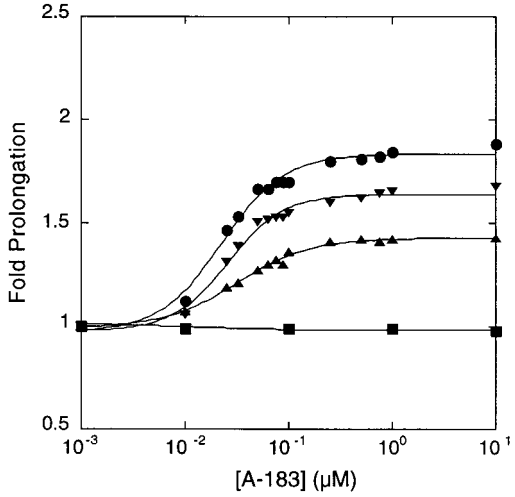

FIGURE 2: Effect of A-183 on the prothrombin time (PT) in different species. The fold prolongation of the clotting times upon initiation by Innovin (human relipidated TF and Ca^{2+}) in the PT assay is plotted versus the concentration of A-183 in citrated pooled normal plasma from human (●), chimpanzee (▼), baboon (▲), and rabbit (■). Uninhibited clotting times for human, chimpanzee, baboon and rabbit were 9.6, 9.3, 10.0, and 8.9 s, respectively.

plasmas with a similar dose dependence to human plasma, although there are differences in the maximal fold-prolongation (Figure 2). This is presumably due to the incomplete inhibition of the rate of FX activation (*30*). Importantly, A-183 did not prolong the PT in rabbit plasma, which negated any possibility of using rabbit thrombosis models. The lack of activity in the rabbit PT assay could be due to a lack of inhibition of rabbit FVIIa or simply a lack of binding.

Since phage bearing peptide A-65, which lacks the two N-terminal Glu residues but has essentially the same affinity for human FVIIa as A-183 (*30*), did not bind to rabbit FVIIa (L. Santell and R. A. Lazarus, unpublished results), we reasoned that the lack of activity in rabbit plasma was due to one or more of the 76 amino acid sequence differences in the protease domains of rabbit and human FVIIa and that these differences could be utilized to identify the exosite where A-183 bound (Figure 3). A total of 70 solvent accessible residues that were different in the human and rabbit FVIIa protease domains were initially incorporated into a series of 14 "rabbitized" mutants of human FVIIa (Figure 3). A-65 phage binding was used as a qualitative measure to screen whether these amino acid sequence differences contributed to binding. All "rabbitized" variants of FVIIa supported A-65 phage binding except FVIIa-r1, FVIIa-r3, and FVIIa-r14, each of which contained multiple amino acid changes. The multiple sequence differences introduced by these mutants were then subdivided into smaller groups of changes from which only FVIIa-r3a and FVIIa-r14b no longer supported binding of A-65 phage (Figure 3). In contrast, subdivision of mutant FVIIa-r1 led to variants r1a-c that were all capable of binding A-65 phage (Figure 3). It is noteworthy that an N-linked glycosylation site is present in FVIIa-r1 at residue 35,[2] which was not present in any of the subsequent FVIIa-r1 mutants. This suggested that glycosylation at this locus prevented A-65 phage from binding. Consistent with this proposal, we have determined that rabbit FVII is glycosylated at this site (L. Santell and R. A. Lazarus, unpublished results). The proximal location of the changes defined by the variants mentioned above suggests a likely peptide binding region defined by the six residues at positions 60b-61 and 250-251.

To further define the A-peptide binding exosite, individual alanine substitutions were introduced at specific residues in this vicinity. The ability of A-100-Z, a recombinant protein comprising A-183 and the Z domain of Protein A for rapid purification and having the same affinity for FVIIa as A-183 (*30*), to inhibit FX activation by these FVIIa alanine mutants was then determined (Figure 4). The specific activity of these mutants for FX activation was generally the same as that for wild-type FVIIa (data not shown), consistent with several of these FVIIa mutants published previously (*16*). A loss in inhibitory activity by the peptide with a given FVIIa mutant thus corresponds to the importance of that particular residue for binding A-100-Z. Inhibition of FX activation by A-100-Z was most affected when Trp 61 and Leu 251 were changed to alanine. Alanine sustitutions at residues Phe 59, Ile 60b, and Ile 90 also impaired A-100-Z activity. It is noteworthy that those residues involved in binding the A-series peptide are distinct from those at the E-peptide binding exosite and the active site (Figure 4). Furthermore, they appear to be distinct from residues involved in binding FX (*16*). Upon the basis of the available crystal structures for FVIIa and TF·FVIIa, we can also place these residues in a structural context, where we find that these residues cluster to form a

[2] The chymotrypsinogen numbering system is used throughout.

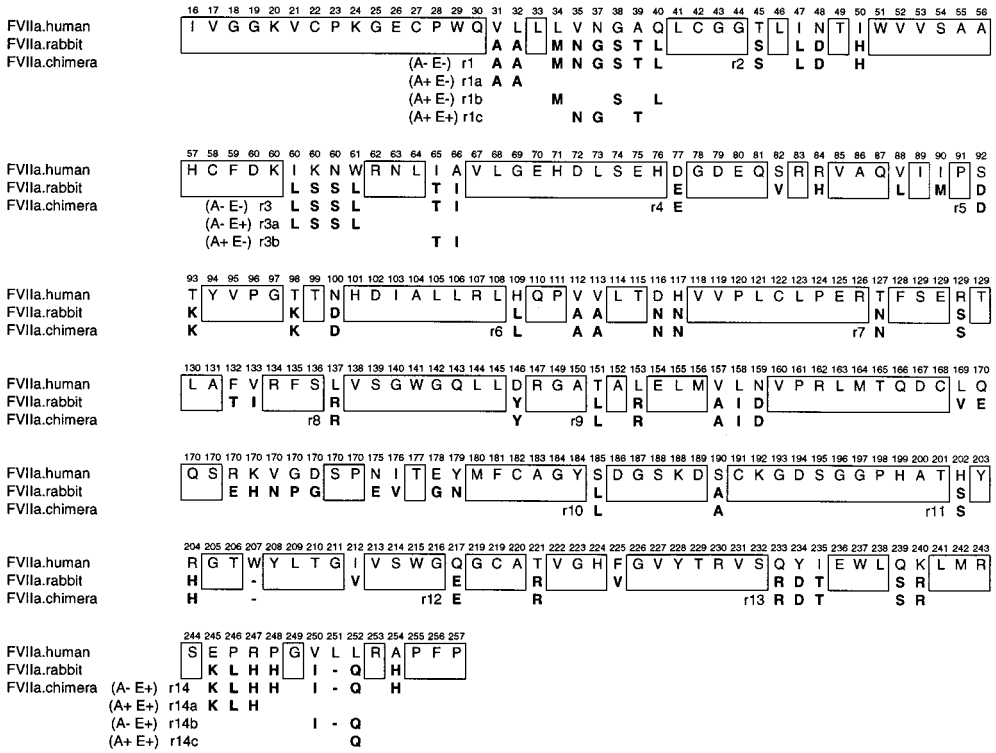

FIGURE 3: Sequence alignment of the human and rabbit FVIIa protease domains. The amino acid sequences from the serine protease domain of human and rabbit FVIIa (*34*) are shown. Identical sequences are boxed and differing sequences are in bold. FVIIa "rabbitized" chimera incorporating rabbit FVIIa sequence into human FVIIa background are depicted as r1, r2, r3, etc., with the specific rabbit residues incorporated shown to the right of r1, r2, r3, etc., and the phenotype ("+" for binding; "−" for no binding) of A-65 phage binding and E-76 phage binding shown in parentheses to the left. Both A-65 and E-76 phage bound to wild type FVIIa and all other mutants where no phenotype is indicated.

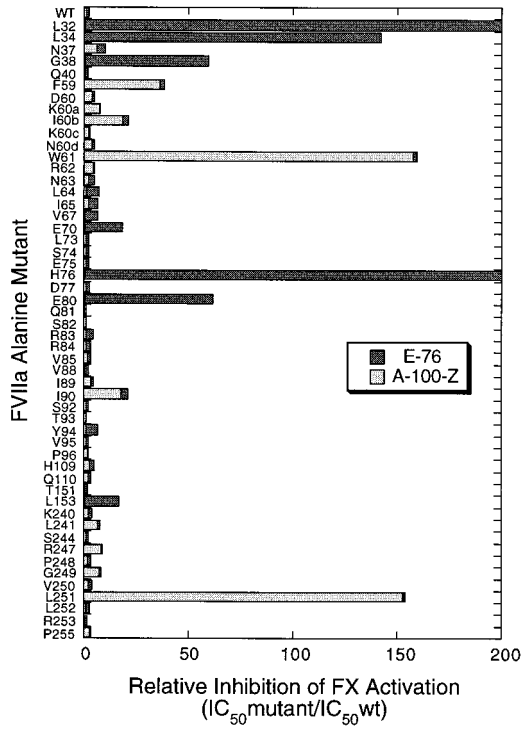

FIGURE 4: Relative inhibition of the TF·FVIIa-catalyzed activation of FX by A-series and E-series peptides with FVIIa alanine mutants. The relative IC_{50} values for the inhibition of FX activation rates by either A-100-Z or E-76 with FVIIa alanine mutants complexed to TF is shown.

binding site for the A-peptide, distinct from both the active site and the E-peptide binding site (vide infra). The protease domain of FVIIa contains a single Ca^{2+} binding site in the 70s loop previously shown to be important for the binding of E-76 (*10*). Consistent with the mutagenesis data which defined the A-peptide binding exosite, we found that varying Ca^{2+} or Mg^{2+} concentrations from 0 to 10 mM had no significant effect on A-183b peptide binding to immobilized FVIIa.

Table 1. Kinetic and Equilibrium Constants for A-183b Binding to Zymogen FVII or FVIIa in the Presence or Absence of TF[a]

	$k_{on} \times 10^{-5}$ (M^{-1} s^{-1})	$k_{off} \times 10^{4}$ (s^{-1})	K_d (nM)
FVII	1.7 ± 0.1	2.4 ± 0.1	1.4 ± 0.1
FVIIa	0.9 ± 0.1	2.5 ± 0.1	2.8 ± 0.2
TF·FVII	1.2 ± 0.1	12.0 ± 1.4	10.0 ± 1.2
TF·FVIIa	2.0 ± 0.2	11.0 ± 0.1	5.5 ± 0.5
TF·FVIIa + E-76	0.7 ± 0.1	6.8 ± 0.3	9.7 ± 0.5

[a] Errors refer to the standard deviation.

Binding Specificity. Direct peptide binding was monitored using surface plasmon resonance. The N-terminus of A-183 was biotinylated (A-183b) enabling its capture on a streptavidin coated chip. The kinetic and equilibrium binding constants of A-183b with various proteins are described in Table 1. A-183b bound to zymogen FVII, FVIIa and TF·FVIIa with fairly similar K_d values of 1.4, 2.8, and 5.5 nM, respectively. In addition, there was essentially no difference in the association rate constants (k_{on}) and a small 4−5-fold increase in the dissociation rate constants (k_{off}), which corresponds to the small decrease in the affinity of A-183b, in the presence of TF (Table 1). Zymogen FVII was still intact following passage over immobilized A-183b as judged

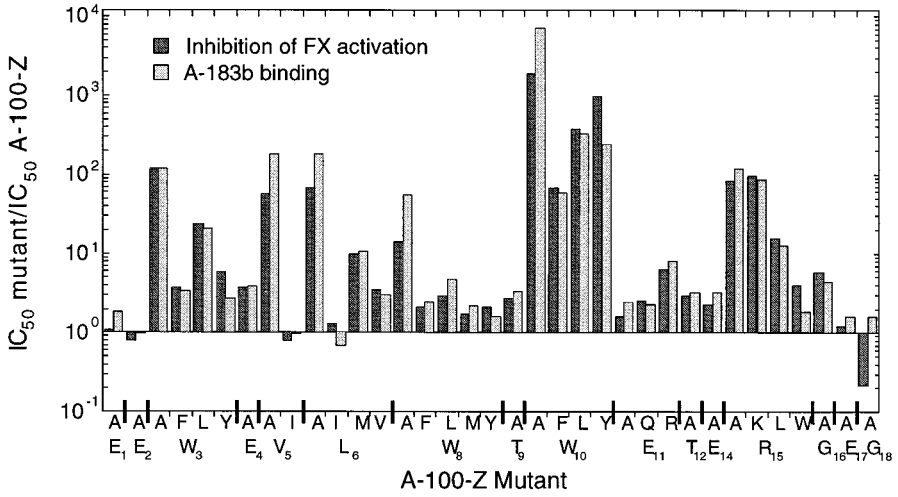

FIGURE 5: Inhibition of TF·FVIIa-catalyzed FX activation and A-183b peptide binding to FVIIa by peptide analogs of A-100-Z. The relative IC_{50} values for inhibition of FX activation by TF·FVIIa or competition with A-183b binding to FVIIa are shown for a series of A-100-Z mutants. All the A-series peptide residues were changed to alanine except for the two cysteines (Cys_7 and Cys_{13}). Amino acids that were shown to be important by alanine substitution were substituted with additional residues as indicated to further assess their structure/function relationship.

by SDS−PAGE analysis. No binding was detected to TF or a number of other serine proteases including thrombin, FXa, FIXa, FXIa, FXIIa, plasma kallikrein, activated protein C, t-PA, and plasmin. Binding of TF·FVIIa to immobilized A-183b was minimally affected by the presence of saturating E-76 which binds at the E-peptide binding exosite (*10*), consistent with earlier observations that the A- and E-peptides bind at distinct exosites. Note that the K_d value for TF·FVIIa is ca. 25-fold higher than the K_i value of 200 pM determined under equilibrium conditions (*30*). We ascribe this difference to solution versus solid phase binding as well as the possibility that biotinylated A-183 immobilized to streptavidin may result in adverse steric consequences which leads to a weaker affinity for FVIIa.

Individual A-Peptide Side Chain Contributions. Alanine substitutions were introduced into A-100-Z and mutants were analyzed for their ability to bind to FVIIa and inhibit FX activation (Figure 5). The loss in inhibition of FX activation was well correlated with a loss in binding to FVIIa. This suggests that binding and inhibition are inseparable despite the fact that the peptides bind at an exosite and could conceivably bind to FVIIa without inhibiting its enzymatic activity. While many positions showed a strong preference for a specific amino acid during maturation (*30*), most of these tolerated alanine substitutions. The disulfide in A-100-Z is critical as evidenced by the replacement of the two cysteines with alanines, which resulted in a variant that was more than 10^4-fold weaker in binding and inhibiting FX activation. Six additional amino acid positions, Trp 3P, Val 5P, Leu 6P, Trp 8P, Trp 10P, and Arg 15P, resulted in a greater than 50-fold decrease in affinity when changed to alanine[3] (Figure 5). Of these, Trp 10P appears to be the most important; an alanine substitution at this position caused a more than 1000-fold decrease in both binding and inhibition of FX activation (Figure 5).

Structure of the A-183·rF7 Complex. We have crystallized A-183 in complex with a zymogen form of FVII termed rF7, which contains only the EGF2 and protease domains (*35*). It is well known that structures of the chymotrypsin family of serine proteases are comprised of two β-barrel subdomains (*3*). Since A-183 binds to the first β-barrel of rF7 (*35*), which undergoes relatively minor changes upon activation and A-183 binds to FVII or FVIIa in the presence or absence of TF with similar affinities (Table 1), we feel it is appropriate to discuss A-183 binding to rF7 in the context of either FVII or FVIIa. Here we discuss the structural aspects of A-183 complexed with rF7; a discussion of the zymogen aspects of this complex is presented elsewhere (*35*).

Consistent with the FVIIa mutagenesis data (Figure 4), A-183 binds at an exosite on the first β-barrel, and not in the active site substrate binding cleft (*35*). The A-peptide binding site is formed on three sides by residues 60a−62, 90−96, and 247−252. When compared to previous structures of FVIIa or TF·FVIIa (*10*, *36*−*39*), significant changes in the first β-barrel caused by A-183 are found only for residues 60a−62 where there is a Cα shift of 5 Å at Trp 61 (Figure 6A).

All peptide side chains except Glu 2P, Thr 9P, Thr 12P, and Glu 14P lose more than 25 Å^2 of accessible surface area each upon complexation with rF7. The greatest effects are seen for Trp 3P, Trp 10P, and Arg 15P, which lose 185, 210, and 151 Å^2, respectively. On a fractional basis, Trp 3P, Cys 7P, Trp 10P, and Cys 13P retain less than 10% of the accessible surface they would have in the middle of an extended tripeptide. On the protein side, the rF7 residues losing more than 25 Å^2 of accessible surface area are Ile 60b, Trp 61, Lys 240, Arg 247, Pro 248, Gly 249, Val 250, Leu 251, Leu 252, Arg 253, and Pro 255.

Peptide A-183 adopts an elongated conformation with an irregular disulfide loop (Figure 6B). There is an extended conformation for residues Glu 1P to Leu 6P. The disulfide between Cys 7P and Cys 13P adopts a (g^+tdg^-t) conformation (*40*), enclosing a loop that, when viewed from the side, looks hook-shaped with its point at Trp 10P. Glu 14P and Arg 15P are in an extended conformation and interact with the N-terminal residues of the peptide through a van der Waals contact between Arg 15P and Leu 6P side chains.

[3] A-100-Z or A-183 residues are designated with a P following the residue number.

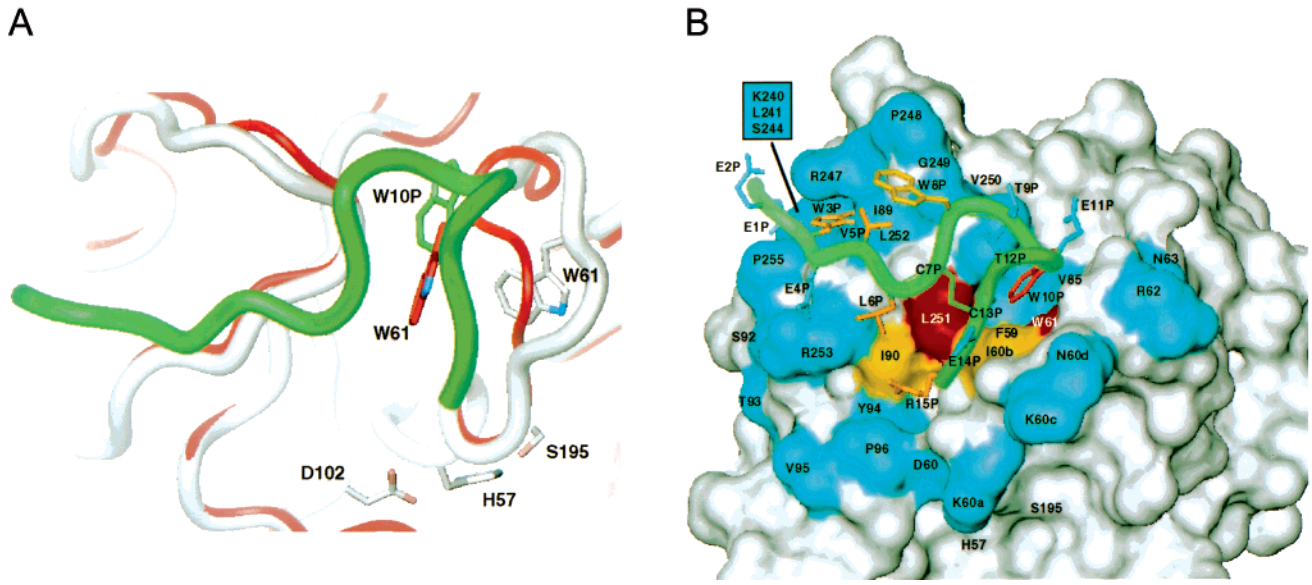

FIGURE 6: Structure activity relationship of the A-183·rF7 complex. (A) The large structural shift of Trp 61 caused by A-183 binding to rF7 is shown. A-183 (green) is complexed with rF7 (grey); FVIIa (red) from TF·FVIIa (*36*) is superimposed onto the rF7 structure. (B) The structure of A-183 (green) complexed with rF7 is shown. The fold increases in the IC_{50} values for A-100-Z inhibition of FX activation for individual alanine substitutions of selected surface-exposed residues of FVIIa are depicted as red (>150), yellow (~20), and blue (~1). A-183 side chains are color coded by the fold-increase in the IC_{50} for inhibition of FX activation for alanine substitution of A-100-Z (red > 1000 , orange = 50−100 , yellow = 10 , blue = 1−3). Approximate positions of active site residues His 57 and Ser 195 (not colored) are shown for reference.

Besides the cystine link, other intrapeptide interactions include a hydrophobic contact between side chains of Val 5P and Trp 8P, and a hydrogen bond between side chains of Thr 9P and Thr 12P. There are also water mediated interactions between the amide nitrogen of Trp 8P and the carbonyl oxygen of Thr 12P, and between carbonyl oxygen atoms of Leu 6P and Glu 14P. The sum of these intrapeptide interactions is insufficient to provide a well-ordered solution structure for the peptide alone (N. Skelton, unpublished results).

Between A-183 and rF7 there are hydrophobic, polar, and charged interactions, including six main chain to main chain hydrogen bonds (Figure 7). We found that A-183b bound to FVIIa with a pH optimum between pH 5 and 10, consistent with the lack of titratable groups in this pH range at the interface; furthermore, the addition of NaCl (up to 1 M) had no significant effect on binding (data not shown). The residue closest to the active site is Arg 15P which hydrogen bonds to the Phe 59 main chain carbonyl oxygen (Figure 7A). The succeeding rF7 residues 60b−62 show the largest change relative to those in FVIIa, experiencing both water mediated and direct main chain to main chain interactions with A-183 (Figures 6 and 7A). The large shift of Trp 61 (~5 Å) creates a deep pocket that accommodates the Trp 10P side chain (Figure 6), which has numerous non-polar contacts with Trp 61, Ile 64, Val 88, Val 250, and Leu 251 as well as a hydrogen bond with the main chain of Val 85 (Figure 7B). There are four hydrogen bonds in a roughly anti-parallel β-sheet arrangement between residues Glu 4P to Cys 7P and Val 250 to Arg 253 (Figure 7C). Trp 3P has hydrophobic contacts with residues Ile 89, Leu 241, Leu 252, and Ala 254, and also a π-stacking arrangement with Arg 247 (Figure 7D). Additional hydrophobic contacts exist between Val 5P and Leu 252, between Leu 6P and residues Leu 251 and Arg 253, between Trp 8P and Pro 248, between Cys 13P and Ile 60b, and between Arg 15P and Ile 60b.

Peptide and Protein Structure-Activity Relationships. The mutational analysis of A-100-Z identified eight functionally and/or structurally important residues that significantly affect binding and inhibition when mutated to alanine. These residues are Trp 3P, Val 5P, Leu 6P, Cys 7P, Trp 8P, Trp 10P, Cys 13P and Arg 15P of which the two cysteines and Trp 10P are the most important (Figure 5). By comparison, a similar set of residues was identified during the soft randomization step of the maturation process (*30*). During peptide maturation, residues Trp 3P, Glu 4P, Val 5P, Cys 7P, Trp 8P, Trp 10P, Glu 11P, and Cys 13P were invariant, suggesting their importance for binding. Although these two sets of residues are not identical, the fact that six of eight residues appear in both supports our view that soft randomization identifies key residues that can be held invariant in later rounds of selection.

The importance of Trp 10P in binding to rF7 is derived from its placement in a pocket lined with the nonpolar side chains of several residues (Figure 7B). Of these, alanine substitutions for Trp 61 and Leu 251 have the largest effects on inhibition of FX activation by A-100-Z (Figure 4). The Trp 10P binding pocket is absent in prior FVIIa structures. Here, it is formed largely as a result of the shift by Trp 61, which, in an approximate way, is replaced by Trp 10P. The size and/or aromatic nature of a tryptophan side chain seems to be important, since Phe substitution for Trp 10P has only a 65-fold decrease in activity, while a Leu substitution has a 380-fold decrease (Figure 5).

Trp 3P is found in what appears to be a beneficial arrangement with the side chain of Arg 247 (Figure 7D), consistent with the 120-fold effect of an alanine substitution of Trp 3P and the negligible effect of a Phe substitution. Although there is also a hydrogen bonding interaction between the Arg 247 side chain and the carbonyl oxygen of Glu 1P, substitution of Arg 247 with alanine surprisingly had a negligible effect. Additionally, none of the protein side

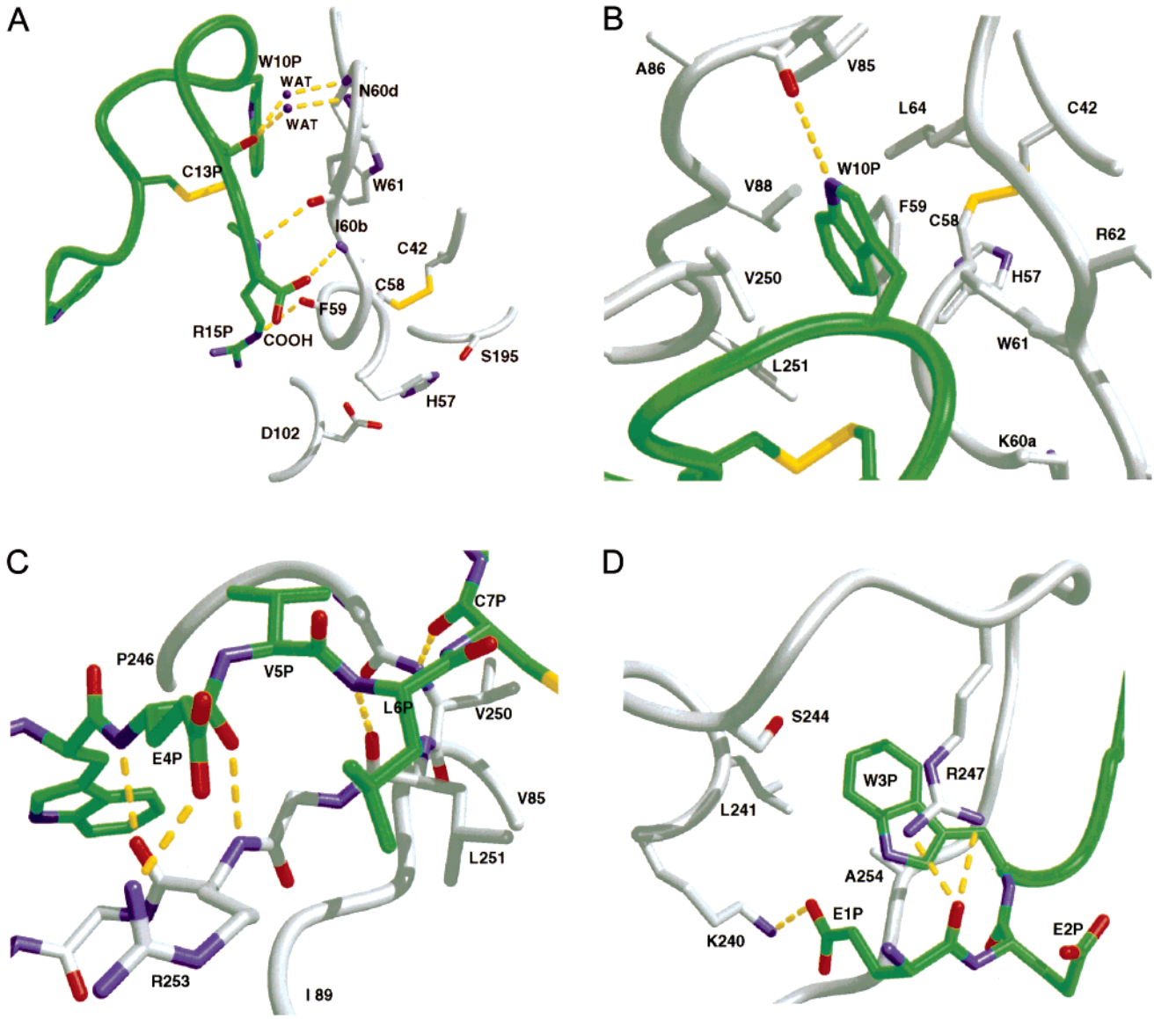

FIGURE 7: Selected interactions between A-183 and rF7. A-183 (green) and rF7 (grey) are depicted with relevant hydrogen bonds (yellow dashes); nitrogen atoms are blue and oxygen atoms are red. (A) Interactions of the C-terminal section of A-183 with the shifted segment of rF7 containing Trp 61, which is close to the enzyme catalytic triad of Asp 102, His 57, and Ser 195. The amide nitrogen atoms of residues Asn 60d and Trp 61 each have a water mediated interaction with the carbonyl oxygen of Cys 13P. The amide nitrogen and the carbonyl oxygen of Ile 60b hydrogen bond to a C-terminal carboxylate oxygen and the amide nitrogen of Arg 15P, respectively. The Arg 15P side chain hydrogen bonds to the carbonyl oxygen of Phe 59. **(B)** The Trp 10P side chain hydrogen bonds to the carbonyl oxygen of Val 85 and is otherwise surrounded by non-polar side chains. (C) Main chain to main chain hydrogen bonds are present between residues Glu 4P, Leu 6P, Cys 7P, and rF7 residues Val 250, Leu 251, and Arg 253. There is also a salt bridge between Glu 4P and Arg 253. (D) The Trp 3P side chain is parallel to and 3.4 Å from the guanidinium moiety of Arg 247. A salt bridge is also formed between Glu 1P and Lys 240.

chains near Arg 247 had large effects when changed to alanine. We hypothesized that Arg 247 to Ala substitution led to relatively larger conformational changes that in some way compensated for the loss of the Arg side chain. We therefore made additional substitutions for Arg 247 and nearby Ala 254. Changing Arg 247 to Glu and Ser resulted in a 32- and 12-fold decrease in activity, respectively. The close contact seen between Trp 3P and Ala 254 is manifested in a 5- and 15-fold decrease in A-100-Z inhibitory activity upon changing Ala 254 to Ser and Thr, respectively. These results tend to confirm the arrangement seen in the crystal structure and leave the behavior of the Arg 247 to Ala substitution as an open question.

Alanine substitution for Arg 15P decreased inhibitory activity by 85-fold. The Arg side chain hydrogen bonds to the carbonyl oxygen of Phe 59 (Figure 7). The C-terminal carboxylate of A-183, which would not be present during the selection process, hydrogen bonds with the main chain nitrogen of Ile 60b. There are also contacts between the Arg 15P side chain and side chains from Ile 60b, Ile 90, and Leu 251. These protein side chains are among the most important for peptide binding. The dominant nonpolar nature of these contacts is indicated by the negligible effect of substitution of Trp for Arg 15P (Figure 5). This constellation of nonpolar contacts also includes the side chain from Leu 6P, consistent with the 70-fold decrease in activity upon alanine substitution

and the negligible effects of its substitution by Ile, Met, or Val. The 50-fold effect of alanine substitution for Val 5P probably relates both to peptide conformational stability, by virtue of the intrapeptide contact with Trp 8P, and to protein interactions with Leu 252.

Mechanism of Inhibition by A-183. Our structure does not present a definitive picture of the mechanism of inhibition by A-183. The inhibitory effect applies to both macromolecular and peptidyl substrates. For inhibition by E-76, we also observed inhibition of macromolecular and peptidyl substrates and had evidence to support both steric and allosteric effects (*10*), including a change in V_{max} likely due to an altered oxyanion hole resulting from a modified hydrogen bonding network. However, the kinetic analysis of A-183 inhibition does not support a change in V_{max} for the smaller chromogenic substrate (*30*), which makes any effect on the oxyanion hole unlikely. Furthermore, in the A-183·rF7 complex the oxyanion hole is not properly formed due to the key role of the amino terminus at Ile16 in FVIIa that is absent in zymogen (*35*). In any case, such a scenario seems unlikely because the A- and E-series peptides bind in different and nonoverlapping exosites.

Peptide A-183 is a partial (hyperbolic) mixed-type inhibitor of FX activation, affecting both the K_m and V_{max}, and a partial competitive inhibitor with a smaller chromogenic substrate, affecting only the K_m (*30*). In both cases, peptide binding affects substrate binding and the inhibition is incomplete. Taken together, this implies that peptide binding induces subtle changes near the active site, i.e., an allosteric effect. The shift of residues Ile 60b−Arg 62 is clearly caused by A-183 binding. The Cα atom of Trp 61 moves by 5 Å, and its side chain by about 6 Å. These shifts are toward residues Val 35 and Leu 41 and have the effect of putting the Trp 61 side chain in approximately the position occupied by the side chain of Ile 60b in TF·FVIIa. The Ile 60b side chain experiences a smaller shift (2 Å at Cα ~3 Å at Cβ) in the opposite direction. These changes may disrupt substrate subsites on the C-terminal side of a substrate's scissile bond, although these subsites are known only by analogy to enzymes where they are better formed and more important for specificity (*3*). In addition, the kinetic differences can be explained by different interactions at these subsites for the two substrates, where allosteric changes in FVIIa could lead to adverse steric consequences causing a V_{max} effect for the macromolecular substrate FX, but not the smaller peptidyl substrate Chromozym t-PA. There are also changes in residues Ser 92 to Asn 100, including a 1 Å shift for the Cα of Thr 99. Changes here have the potential to influence the S2 subsite on the N-terminal side of the scissile bond. However, this section of the protein is between the A-183 exosite and the strongly shifted residues Lys 170d−Pro 170i that are part of zymogen-related changes, preventing a straightforward assignment of cause and effect.

Exosites as Targets for Inhibition. The most common approach to develop enzyme inhibitors has been to attack the active site directly. While the notion of allosteric regulation of proteins is well documented, there has been relatively little effort directed towards inhibiting enzymes via allosteric mechanisms from exosites (*41*, *42*). Both experimental and theoretical aspects of the allosteric modulation of serine proteases, and in particular thrombin and FVIIa, have been addressed (*26*, *43*−*45*). The role of exosites in macromolecular substrate interactions for both the prothrombinase and extrinsic Xase complexes has recently revealed their importance for these enzymes (*18*, *24*, *25*, *46*). A potential advantage of inhibiting enzymes via exosites includes the ability to regulate inhibition with greater specificity. However, the ability to inhibit via exosites is not strictly limited to the enzyme as the target. In a recent noteworthy report on the mechanism of action of recombinant nematode anticoagulant protein rNAPc2, Bergum et al. have shown that rNAPc2 inhibits TF·FVIIa by first binding to an exosite on the substrate zymogen FX or the product FXa before presenting a canonical inhibitory loop into the active site of FVIIa (*47*).

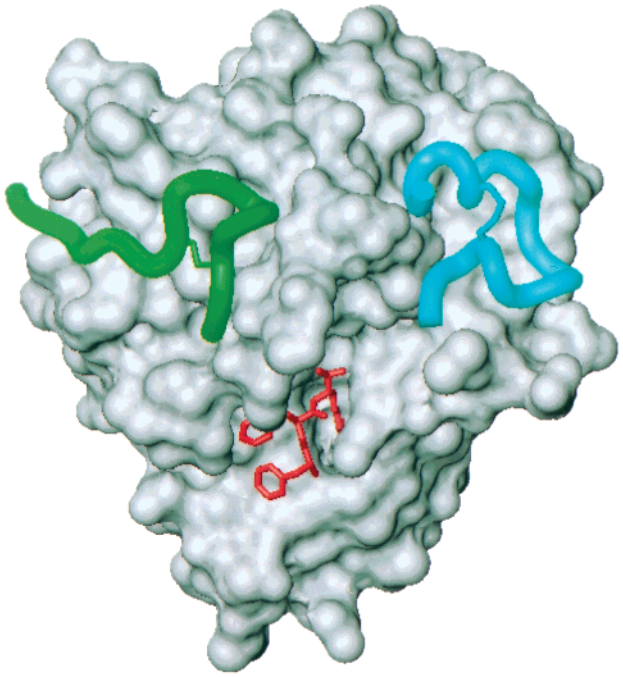

FIGURE 8: FVIIa binding sites. The distinct regions of the peptide binding exosites for A-183 (green) and E-76 (blue) are shown with the solvent accessible surface of the protease domain of FVIIa, which was modeled by combining the first β-barrel from A-183·rF7 with the second β-barrel from the E-76·FVIIa complex (*10*). The active site region from the E-76·FVIIa complex (*10*), covalently modified with D-Phe-L-Phe-L-Arg-chloromethyl ketone (red) is also shown.

CONCLUSIONS

Structural comparison of the A-peptide binding exosite described in this work with either the E-peptide binding exosite or the active site clearly demonstrates that these three sites are quite distinct (Figure 8). Functional comparison of these sites shows us that potent inhibition can be accomplished by binding to any of these sites. We were initially surprised that the phage diversity approach we took resulted in peptides that were such potent and selective inhibitors (*10*). We are even more struck by the fact that there are now unrelated peptides acting at novel and distinct binding exosites that display both potent and selective inhibition. The success at obtaining a second series of potent and selective inhibitors lends support to the notion that the approach we have taken represents a paradigm for developing inhibitors of serine proteases and perhaps other enzymes as well.

ACKNOWLEDGMENT

We are grateful to D. Kirchhofer and R. Kelley for a critical reading of this manuscript and many helpful discussions. We thank R. Kelley and M. O'Connell for TF, FVII, and FVIIa, S. Bullens and R. Smyth for clotting assay data, M. Ultsch for crystallographic data on the A-183•rF7 complex, C. Quan, J. Tom, and M. Struble for peptide synthesis, M. Beresini and L. Caris for A-183b ELISA assay data and helpful discussions, P. Jhurani, P. Ng, and M. Vasser for DNA synthesis, A. Zhong, M. Hamner, and A. Goddard for DNA sequencing, D. Stafford and J. Toomey for plasmids encoding FVII and FVII/FIX chimeras, and R. Artis, N. Skelton, and C. Refino for helpful discussions. We also acknowledge Thomas Earnst and Keith Henderson of ALS for data collection assistance. The Advanced Light Source is supported by the Director, Office of Basic Energy Sciences, Materials Science Division of the U. S. Department of Energy under Contract DE-AC03-76SF00098 at the Lawrence Berkeley National Laboratory. We would like to acknowledge A. de Vos for his support.

REFERENCES

1. Neurath, H. (1984) *Science 224*, 350−357.
2. Barrett, A. J., Rawlings, N. D., and Woessner, J. F. (1998) in *Handbook of Proteolytic Enzymes*, Academic Press, London.
3. Perona, J. J., and Craik, C. S. (1995) *Protein Sci. 4*, 337−360.
4. Siezen, R. J., and Leunissen, J. A. M. (1997) *Protein Sci. 6*, 501−523.
5. Davie, E. W., Fujikawa, K., and Kisiel, W. (1991) *Biochemistry 30*, 10363−10370.
6. Mann, K. G. (1999) *Thromb. Haemost. 82*, 165−174.
7. Dennis, M. S., and Lazarus, R. A. (1994) *J. Biol. Chem. 269*, 22129−22136.
8. Dennis, M. S., and Lazarus, R. A. (1994) *J. Biol. Chem. 269*, 22137−22144.
9. Lee, G. F., Lazarus, R. A., and Kelley, R. F. (1997) *Biochemistry 36*, 5607−5611.
10. Dennis, M. S., Eigenbrot, C., Skelton, N. J., Ultsch, M. H., Santell, L., Dwyer, M. A., O'Connell, M. P., and Lazarus, R. A. (2000) *Nature 404*, 465−470.
11. Gallagher, K. P., Mertz, T. E., Chi, L., Rubin, J. R., and Uprichard, A. C. G. (1999) in *Antithrombotics* (Uprichard, A. C. G., and Gallagher, K. P., Eds.) pp 421−445, Springer-Verlag, Berlin.
12. Broze, G. J., Jr. (1995) *Annu. Rev. Med. 46*, 103−112.
13. Rapaport, S. I., and Rao, L. V. M. (1995) *Thromb. Haemost. 74*, 7−17.
14. Higashi, S., and Iwanaga, S. (1998) *Int. J. Hematol. 67*, 229−241.
15. Ruf, W. (1994) *Biochemistry 1994*, 11631−11636.
16. Dickinson, C. D., Kelly, C. R., and Ruf, W. (1996) *Proc. Natl. Acad. Sci. U.S.A. 93*, 14379−14384.
17. Edgington, T. S., Dickinson, C. D., and Ruf, W. (1997) *Thromb. Haemost. 78*, 401−405.
18. Dickinson, C. D., Shobe, J., and Ruf, W. (1998) *J. Mol. Biol. 277*, 959−971.
19. Ruf, W., Shobe, J., Rao, S. M., Dickinson, C. D., Olson, A., and Edgington, T. S. (1999) *Biochemistry 38*, 1957−1966.
20. Roy, S., Hass, P. E., Bourell, J. H., Henzel, W. J., and Vehar, G. A. (1991) *J. Biol. Chem. 266*, 22063−22066.
21. Ruf, W., Miles, D. J., Rehemtulla, A., and Edgington, T. S. (1992) *J. Biol. Chem. 267*, 6375−6381.
22. Huang, Q., Neuenschwander, P. F., Rezaie, A. R., and Morrissey, J. H. (1996) *J. Biol. Chem. 271*, 21752−21757.
23. Kirchhofer, D., Lipari, M. T., Moran, P., Eigenbrot, C., and Kelley, R. F. (2000) *Biochemistry 39*, 7380−7387.
24. Shobe, J., Dickinson, C. D., Edgington, T. S., and Ruf, W. (1999) *J. Biol. Chem. 274*, 24171−24175.
25. Baugh, R. J., Dickinson, C. D., Ruf, W., and Krishnaswamy, S. (2000) *Biochemistry 275*, 28826−28833.
26. Stubbs, M. T., and Bode, W. (1993) *Thromb. Res. 69*, 1−58.
27. Stubbs, M. T., and Bode, W. (1995) *Trends Biochem. Sci. 20*, 23−28.
28. Skrzypczak-Jankun, E., Carperos, V. E., Ravichandran, K. G., Tulinsky, A., Westbrook, M., and Maraganore, J. M. (1991) *J. Mol. Biol. 221*, 1379−1393.
29. Naski, M. C., Fenton, J. W. I., Maraganore, J. M., Olson, S. T., and Shafer, J. A. (1990) *J. Biol. Chem. 265*, 13484−13489.
30. Dennis, M. S., Roberge, M., Quan, C., and Lazarus, R. A. (2001) *Biochemistry 40* 9513−9521.
31. Starovasnik, M. A., O'Connell, M. P., Fairbrother, W. J., and Kelley, R. F. (1999) *Protein Sci. 8*, 1423−1431.
32. Toomey, J. R., Smith, K. J., and Stafford, D. W. (1991) *J. Biol. Chem. 266*, 19198−19202.
33. Kunkel, T. A., Roberts, J. D., and Zakour, R. A. (1987) *Methods Enzymol. 154*, 367−382.
34. Ruiz, S. M., Sridhara, S., Blajchman, M. A., and Clarke, B. J. (2000) *Thromb. Res. 98*, 203−211.
35. Eigenbrot, C., Kirchhofer, D., Dennis, M. S., Santell, L., Lazarus, R. A., Stamos, J., and Ultsch, M. H. (2001) *Structure 9*, 627−636.
36. Banner, D. W., D'Arcy, A., Chène, C., Winkler, F. K., Guha, A., Konigsberg, W. H., Nemerson, Y., and Kirchhofer, D. (1996) *Nature 380*, 41−46.
37. Kemball-Cook, G., Johnson, D. J. D., Tuddenham, E. G. D., and Harlos, K. (1999) *J. Struct. Biol. 127*, 213−223.
38. Pike, A. C. W., Brzozowski, A. M., Roberts, S. M., Olsen, O. H., and Persson, E. (1999) *Proc. Natl. Acad. Sci. U.S.A. 96*, 8925−8930.
39. Zhang, E., St. Charles, R., and Tulinsky, A. (1999) *J. Mol. Biol. 285*, 2089−2104.
40. Harrison, P. M., and Sternberg, M. J. (1996) *J. Mol. Biol. 264*, 603−623.
41. DeDecker, B. S. (2000) *Chem. Biol. 7*, R103−R107.
42. Banner, D. W. (2000) *Nature 404*, 449−450.
43. Duffy, E. J., Angliker, H., Le Bonniec, B. F., and Stone, S. R. (1997) *Biochem. J. 321*, 361−365.
44. Di Cera, E., Hopfner, K. P., and Dang, Q. D. (1996) *Biophys. J. 70*, 174−181.
45. Ruf, W., and Dickinson, C. D. (1998) *Trends Cardiovasc. Med. 8*, 350−356.
46. Krishnaswamy, S., and Betz, A. (1997) *Biochemistry 36*, 12080−12086.
47. Bergum, P. W., Cruikshank, A., Maki, S. L., Kelley, C. R., Ruf, W., and Vlasuk, G. P. (2001) *J. Biol. Chem. 276*, 10063−10071.

BI010592D